RayFlex: Inducing Weight Perception through Raycast Pseudo-Haptics in Virtual Reality

Yushi Wei, Sen Zhang, Rongkai Shi, Simon Fong, Pan Hui, and Hai-Ning Liang

Abstract—Weight perception is essential for delivering compelling and realistic object interaction in VR systems. While existing pseudo-haptic techniques have enabled users to perceive virtual object weight without physical actuation, their application has primarily been limited to near-field, direct hand interaction. As VR systems continue to advance in fidelity and versatility, interactions with objects beyond arm's reach are becoming increasingly common. However, how weight perception can be introduced into such remote interactions, and whether it can enhance user immersion and experience, remains underexplored. To bridge this gap, we present RayFlex, a pseudo-haptic technique that conveys object weight in raycasting-based interaction through visual displacement and dynamic ray deformation. The technique was evaluated in two user studies, which examined its effectiveness in supporting weight discrimination and its impact on user experience across different interaction contexts. Results indicate that RayFlex leads to significant improvements in perceived realism, presence, and satisfaction, while maintaining usability. From the results, we derived two implications and an application guideline that can help design future VR systems.

Index Terms—Weight perception, pseudo-haptics, remote object interaction, virtual reality, interaction design, user study

1 Introduction

Today's VR systems enable users to interact with virtual content flexibly, whether it is within arm's reach or beyond [26, 52]. To support such interactions efficiently, a range of techniques has been introduced [16, 35, 49]. Among these, direct hand interaction and raycasting have been widely adopted as primary techniques for selecting and manipulating virtual objects in near-field and far-field contexts, respectively—with the former relying on physical hand reach and the latter enabling distance control through a projected virtual ray [26]. Building on these foundational techniques, subsequent work has introduced refinements to foster greater immersion and enhance overall user experience. One prominent approach aims to approximate real-world physicality by endowing virtual objects with perceptually meaningful properties, such as weight, compliance, and friction, to support consistent perception and interaction [39]. Across these properties, weight has been consistently identified as a key contributor to users' sense of presence, engagement, and perceived realism [28, 32, 38, 42]. To evoke this sensation, prior work has employed **pseudo-haptic feedback**, a class of techniques that induce haptic sensations by deliberately manipulating visual feedback rather than providing physical force input. In the context of weight perception, pseudo-haptic feedback is typically realized by adjusting the motion dynamics of virtual objects in response to user interactions, such as introducing motion delays or modifying control-display ratios. By relying solely on visual cues, this approach can create a convincing illusion of weight without requiring force-feedback hardware, offering advantages such as high scalability, ease of deployment, and low implementation cost [13].

While pseudo-haptic weight feedback has demonstrated effectiveness in enhancing presence and realism, its use has been primarily verified in direct hand interaction. In scenarios involving interactions with distant objects, such as those using raycasting, its applicability remains underexplored. Moreover, given that VR systems continue to improve in fidelity and increasingly support interactions beyond arm's reach [26], incorporating weight-related cues into these contexts is becoming increasingly relevant and presents a promising direction for enhancing user engagement and perceptual coherence. However, extending pseudo-haptics to these contexts poses two key challenges. First, unlike direct manipulation, raycasting lacks an intuitive real-world analogue (e.g., grasping or lifting), making it harder for users to interpret purely visual cues as weight indicators. Second, the method for achieving coherent mapping between physical input and virtual response in such a context remains unclear; any mismatch between these layers can disrupt embodiment and immersion, which could ultimately erode presence and interaction quality [13, 19, 33].

To bridge this gap, this work introduces **RayFlex**, a raycasting-based interaction technique that conveys weight perception without haptic devices. RayFlex integrates two mechanisms: a visual displacement model, where selected objects exhibit mass-dependent lag and vertical offset to mimic inertia and gravity, and a dynamic ray visualization that bends in proportion to the object's virtual weight, serving as a continuous visual cue of heaviness. To guide its design, we first reviewed prior work on weight perception simulation and interaction with distant objects in VR. (Sec. 2). Drawing on insights from this review and relevant physical principles, the design considerations and implementation are detailed in Sec. 3. We then conducted a first study to examine its effectiveness in conveying weight sensation and to analyze the rationale behind its core components (Sec. 4). A second study further evaluated the complete technique against standard raycasting across two VR tasks, focusing on user experience and preferences for integrating weight perception into distant interaction (Sec. 5). Results from both studies indicate that RayFlex conveys distinguishable weight sensations and improves presence and overall interaction experience. Based on these findings, we derived two design recommendations and a practical guideline to support the future development and deployment of RayFlex (Sec. 6).

In summary, the primary contributions of our work include: **(1)** A novel technique that integrates weight sensation into raycasting interaction through adjustable parameters, enabling adaptation to diverse interaction scenarios and improving user immersion and experience. **(2)** Two user studies that empirically evaluate the effectiveness of the proposed technique and offer actionable design recommendations and application guidelines for future researchers, designers, and practitioners. **(3)** An open-source implementation of RayFlex to facilitate future research and adoption.[1]

- *Yushi Wei, Sen Zhang, Rongkai Shi, Pan Hui, and Hai-Ning Liang are with the Computational Media and Arts Thrust (CMA), The Hong Kong University of Science and Technology (Guangzhou), Guangzhou, China.*
- *Simon Fong is with the Department of Computer and Information Science, University of Macau, Macau SAR, China.*
- *Hai-Ning Liang is also with the Division of Arts and Machine Creativity, The Hong Kong University of Science and Technology, Hong Kong SAR, China.*
- *Corresponding author: Hai-Ning Liang (hainingliang@hkust-gz.edu.cn).*

Received 12 September 2025; revised 16 January 2026; accepted 23 January 2026. Date of publication 1 April 2026; date of current version 12 May 2026.
Digital Object Identifier no. 10.1109/TVCG.2026.3679883

[1] Unity demo program: github.com/yushiwei21-lab/IEEE-VR-RayFlex.

2 Related Work

This section first reviews existing approaches to enabling weight perception in VR (Sec. 2.1). It then examines the role of raycasting as a fundamental interaction technique, outlining both its advantages in supporting interaction with distant objects and its limitations in conveying weight-related perceptual experience (Sec. 2.2).

2.1 Simulation of Weight in Virtual Reality

Simulating weight sensation in VR remains a longstanding challenge because current VR systems lack physical force feedback to mimic the gravitational effects of virtual objects. This limitation makes it difficult for users to perceive mass during mid-air interactions and constrains the realism and expressiveness of VR interaction [39]. To address this issue, one prominent class of solutions focuses on haptic devices that can provide real force feedback through mechanical actuation. These haptic techniques span a wide range of designs, targeting different parts of the body such as the feet [1, 56], hands [28, 36, 42], or fingertips [6], and employ strategies like dynamic mass shifting [28, 42, 54], structural deformation [15], or resistance modulation [37, 55]. While effective in delivering realistic sensations, these devices often entail high cost, cumbersome setup, and limited generalizability [38], making them less suitable for scalable or everyday VR applications.

To overcome the limitations of hardware-based techniques, recent research has increasingly explored pseudo-haptic feedback-software-driven illusions that mainly leverage visual perception to simulate physical properties without requiring mechanical actuation [2, 7, 39]. These techniques have shown promising results in conveying surface-level tactile cues such as stiffness [21], texture [8], and friction [22]. However, simulating weight through pseudo-haptics remains challenging due to its strong association with motor effort and inertial resistance-phenomena that are difficult to emulate without physical force feedback [9, 18].

To address this, researchers have proposed a range of strategies, with one of the most widely adopted being control/display (C/D) ratio modulation [29, 38], defined as the ratio $\alpha = D'/D$ between visual and physical displacement, where D represents the user's physical input displacement and D' denotes the corresponding displacement of the controlled object in the visual display. When $\alpha < 1$, the reduced response mimics increased heaviness; when $\alpha > 1$, the effect is reversed [30]. This approach has been successfully applied to tasks such as grasping [2], rotation [53], and lifting [33], and functions across input modalities ranging from hand-held controllers to bare-hand tracking [14, 38].

Beyond the C/D ratio modulation, researchers have explored additional visual displacement strategies for simulating weight, notably tracking delay and vertical offset. A tracking delay introduces a temporal mismatch between the user's physical input and the corresponding visual response [13]. When the virtual object no longer instantly follows the hand, it appears to lag and then catch up, which users intuitively interpret as inertial resistance or increased weight [17]. Studies show this method to be effective in continuous actions like lifting or dragging, where even subtle timing discrepancies are perceptually salient [13, 17, 41]. A vertical offset, on the other hand, manipulates the spatial alignment between the real and virtual hands along the gravity axis [32]. Rendering the virtual hand slightly above or below the physical one modulates the perceived lifting effort: upward offsets increase the sense of heaviness, while downward offsets make objects seem light [13, 48]. Unlike the C/D ratio, which uniformly scales motion in all directions, vertical offset introduces directional discrepancies aligned with gravity, leveraging proprioceptive expectations to produce effort-based weight illusions.

While techniques such as C/D ratio modulation, tracking delay, and vertical offset have demonstrated effectiveness in eliciting weight-related illusions [13, 19, 33], two key limitations remain. First, these techniques often bring perceptual and usability challenges in scenarios that require continuous hand-object coupling. In such contexts, spatial misalignments between the real and virtual hands can disrupt motor coordination and weaken the sense of body ownership [13, 33]. Second, existing approaches were developed for interaction within arm's length, where users engage with virtual objects through direct manipulation. However, interaction in VR is often for objects located beyond users' arm's reach and relies on approaches based on raycasting. Due to the fundamental differences in interaction dynamics, this interaction with distant objects presents new challenges for designing suitable pseudo-haptic techniques for such contexts.

2.2 Raycasting-based Interaction

Raycasting is one of the most widely used techniques for interacting with distant objects in virtual environments [3]. A virtual ray is emitted from a user-controlled origin and extends into the scene. When the ray intersects an interactable object, the user can select or manipulate it via the ray [4].

To better understand and improve this technique, prior work has broken down the ray into three components: the origin, the visual ray segment, and the endpoint [51]. Each component has been shown to significantly influence users' performance and subjective experience, as well as inform the design of the techniques. Specifically, the origin denotes the body part from which the ray is emitted, such as the head [11], torso [16], or hand [26, 51], with each part offering distinct trade-offs in terms of precision, control, and spatial awareness. The ray segment, which extends from the origin, serves as the visual and functional link to the endpoint object, and its visual form has been shown to significantly impact both effectiveness and usability. For example, curved rays can facilitate the selection of occluded targets [12], while fan-shaped rays better accommodate imprecise pointing in dense layouts [43]. However, increased visual complexity may introduce distraction and reduce interaction clarity [20, 24], highlighting the importance of tailoring ray segment design to specific task demands. Finally, the endpoint-the object being interacted with-plays a key role in shaping the demands and effectiveness of raycasting. Its properties (e.g., size, distribution, depth) and the broader interaction context (e.g., realistic vs. abstract tasks) jointly shape user expectations and influence interaction outcomes [44, 51]. A mismatch between endpoint characteristics and the interaction design can undermine usability and break immersion [45].

Beyond its internal components, comparative studies have further demonstrated the overall effectiveness of raycasting relative to other interaction methods, such as virtual hand [49, 50], with advantages including reduced physical effort, improved accuracy, and faster interaction [26]. However, its limitations have also been well-documented, such as the lack of intuitive interaction and reduced immersion [5, 25, 27]. To address these issues and support more natural interaction experiences, incorporating weight perception into raycasting-based interaction offers a promising avenue, as previous research has shown its potential to enhance user immersion and presence [39]. Nevertheless, current raycasting techniques remain limited in their ability to convey such physical properties. This limitation primarily arises from the absence of real-world analogues and motor actions-such as grasping and lifting-that users typically rely on to infer object weight in both virtual hand interaction and everyday life [13, 31]. As a result, reproducing the sensation of weight through raycasting remains inherently challenging due to the lack of real-world references. Moreover, existing designs developed for virtual hand interaction cannot be directly applied to raycasting-based techniques because of the fundamental differences in interaction paradigms and user input dynamics.

3 RayFlex

This section presents the design of RayFlex, a pseudo-haptic feedback technique that enables raycasting-based interaction to convey the sensation of object weight. We begin by discussing the choice of the visual displacement area (Sec. 3.1), then introduce the displacement mechanism developed to control object motion (Sec. 3.2); and finally, we redesign the ray visualization to reinforce the sense of weight (Sec. 3.3). Together, these components form the complete design of RayFlex.

3.1 Visual Displacement Area

Prior work on pseudo-haptic feedback for virtual hand interaction has shown that visually displacing hand motion can effectively elicit weight perception. However, such manipulations may also disrupt embodiment

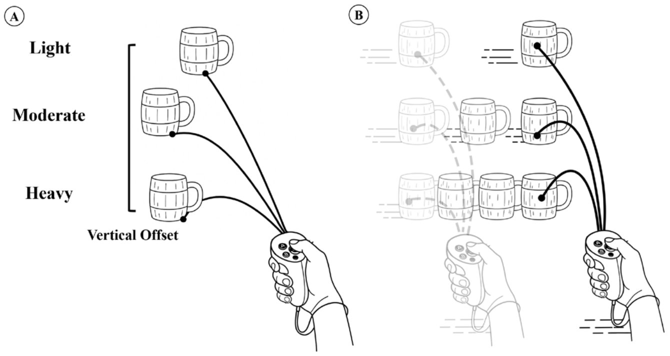

Fig. 1: Illustration of RayFlex in raycasting interaction with three weight levels (light, moderate, heavy). (A) In the static state, heavier objects result in a larger vertical offset. (B) During lateral dragging, heavier objects show a greater motion delay.

by introducing spatial mismatches between the real and virtual hands, resulting in reduced body ownership and presence (see Sec. 2.1). In raycasting-based interaction, although direct hand involvement (e.g., grasping) is reduced, perceptual inconsistencies may still arise when visual feedback fails to align with user motion or intent. Therefore, designing pseudo-haptic feedback for raycasting requires careful coordination between user actions and virtual responses to preserve a coherent sense of embodiment.

To support such coordination, a key design choice involves determining where visual displacement should be applied within the raycasting structure, without compromising presence. As discussed in Sec. 2.2, raycasting typically consists of three elements: the origin, the visual ray, and the endpoint. To preserve embodiment and avoid mismatches between the user's physical hand and its virtual representation, visual displacement is applied solely to the object at the endpoint, thereby excluding hand motion from visual distortion.

3.2 Visual Displacement Mechanism

As the central mechanism for conveying object weight, visual displacement plays a key role in the RayFlex. Accordingly, we model the selected virtual object as a point mass connected to the controller via the ray, using a mass-spring-damper (MSD) system. Specifically, instead of snapping immediately to the ideal position along the controller's forward axis, denoted as $\vec{P}_2^{\text{ideal}}$, the object follows a delayed and vertically offset trajectory (see Fig. 1). Both effects scale with its virtual mass, mimicking the inertial behavior of a weighted object under tension.

This mass-dependent lag and offset result from the interplay of three canonical forces defined in the MSD model. The first component is gravity, which applies a constant downward force on the object:

$$F_g = m\,g, \tag{1}$$

where m is the virtual mass (in kilograms), and g is the gravitational acceleration vector, typically defined as $\vec{g} = (0, -9.81, 0), \mathrm{m/s^2}$, pointing downward.

Second, a restoring spring force proportional to the displacement pulls the object toward its original ray-aligned target position.

$$F_s = -k\left(\vec{P}_2^{\text{actual}}(t) - \vec{P}_2^{\text{ideal}}(t)\right), \tag{2}$$

where k is the linear spring stiffness coefficient $[\mathrm{N/m}]$, $\vec{P}_2^{\text{ideal}}(t)$ denotes the ideal target position defined by the ray, and $\vec{P}_2^{\text{actual}}(t)$ is the object's current position.

Finally, a velocity-dependent damping force acts to resist motion and eliminate oscillations:

$$F_d = -c\,\dot{\vec{P}}_2^{\text{actual}}(t), \quad \text{where } c = 2\zeta\sqrt{km}, \tag{3}$$

where ζ denotes the damping ratio. The critical damping condition is achieved by setting $\zeta = 1$, enabling rapid, non-oscillatory convergence to the target.

Together, gravity, spring, and damping forces determine the net force acting on the object at each moment. We describe the resulting motion using Newton's second law—we relate force to mass and acceleration and derive a second-order differential equation that governs the object's trajectory under these combined forces:

$$m\,\ddot{\vec{P}}_2^{\text{actual}}(t) + c\,\dot{\vec{P}}_2^{\text{actual}}(t) + k\left(\vec{P}_2^{\text{actual}}(t) - \vec{P}_2^{\text{ideal}}(t)\right) = m\vec{g}, \tag{4}$$

This formulation captures the interplay between inertia, elastic restoration, and damping, driving the object's trajectory in response to user motion and enhancing the sense of weight through physically plausible behavior.

Finally, as closed-form solutions to Eq. (4) are infeasible for real-time computation, we employ a time-stepping numerical integration method. The equation is discretized using a fixed timestep Δt and solved via the semi-implicit Euler method, a first-order integration scheme known for its improved stability in dynamic physical systems:

$$\begin{aligned} \vec{v}_{t+\Delta t} &= \vec{v}_t + \frac{\Delta t}{m}\left(\vec{F}_g + \vec{F}_s + \vec{F}_d\right), \\ \vec{P}_{2\,t+\Delta t}^{\text{actual}} &= \vec{P}_{2t}^{\text{actual}} + \Delta t\,\vec{v}_{t+\Delta t} \end{aligned} \tag{5}$$

3.3 Ray Visualization

In addition to the visual displacement of the object, we further considered the role of the ray itself, which serves as a direct visual cue connecting the origin and the object in the raycasting system. We therefore redesigned its appearance to better convey the sense of object weight. Unlike conventional rays with fixed shapes, which are either straight or uniformly curved, we introduce a ray with dynamic curvature that visually adapts to the weight of the selected object and bends only when user motion causes a visible lag between the ray and the object. This design draws on real-world analogies; the ray visually bends under simulated heavy loads, resembling the deflection of a fishing rod under tension (see Fig. 1).

Specifically, we represent the ray as a quadratic Bézier curve and update its control points each frame based on the controller's world-space pose and the displacement-adjusted target position. To compute the curve geometry, we define the following quantities: $\vec{P}_0(t) \in \mathbb{R}^3$ denotes the controller's position at time t, and $\vec{f}(t) \in \mathbb{R}^3$ is its normalized forward direction. The ray has a fixed length $L > 0$, typically defined as the distance between the controller and the object at the moment of selection. In the absence of displacement, the ray terminates at the ideal position:

$$\vec{P}_2^{\text{ideal}}(t) = \vec{P}_0(t) + L\vec{f}(t) \tag{6}$$

When displacement is employed, the object's rendered position is displaced relative to $\vec{P}_2^{\text{ideal}}(t)$, lagging for heavier objects. We denote this adjusted position as $\vec{P}_2^{\text{actual}}(t)$ and define the resulting deviation as:

$$\vec{\Delta}(t) = \vec{P}_2^{\text{ideal}}(t) - \vec{P}_2^{\text{actual}}(t) \tag{7}$$

Next, the Bézier control point $\vec{P}_1(t)$ is computed such that the ray remains straight when $\vec{\Delta}(t) = 0$ and bends proportionally otherwise. The scaling factor s is empirically chosen to ensure the curvature is visible yet not exaggerated.

$$\vec{P}_1(t) = \frac{\vec{P}_0(t) + \vec{P}_2^{\text{ideal}}(t)}{2} + s\vec{\Delta}(t) \tag{8}$$

By substituting $\vec{P}_0(t)$, $\vec{P}_1(t)$, and $\vec{P}_2^{\text{actual}}(t)$ into the standard quadratic Bézier curve equation, we obtain:

$$B(t,u) = (1-u)^2\vec{P}_0(t) + 2u(1-u)\vec{P}_1(t) + u^2\vec{P}_2^{\text{actual}}(t), \quad u \in [0,1]. \tag{9}$$

Here, $u \in [0,1]$ parameterizes the curve from $\vec{P}_0(t)$ to $\vec{P}_2^{\text{actual}}(t)$.

As the user tilts or lifts the controller, the upward component of $\vec{f}(t)$ increases, amplifying $\vec{\Delta}(t)$ and pushing $\vec{P}_1(t)$ farther from the midpoint. This deformation causes the ray to sag under heavier loads, potentially reinforcing the visual illusion of weight.

4 Study 1: Validating the Effectiveness of RayFlex for Weight Perception

In the first study, we investigated the performance and user experience of RayFlex for enhancing participants' weight perception in VR. Specifically, we answered two research questions (**RQ#**):

RQ1. How does RayFlex influence users' perception of virtual object weight? RayFlex is designed to simulate the sensation of weight in distant-object interaction by modulating visual cues. Unlike virtual hand interaction, raycasting lacks visual indications of physical contact and relevant motor actions-cues typically relied upon in real-world weight perception. This abstraction complicates the delivery of weight cues, making it important to assess whether RayFlex's visual modulation alone can elicit a consistent and reliable sense of weight.

RQ2. How does dynamic ray deformation influence users' experience in RayFlex? In RayFlex, besides the visual displacement between the origin and the object, the ray itself is treated as a visual cue for conveying the weight sensation. However, prior research has highlighted that overly complex ray visualizations may introduce visual distraction and reduce user experience (see Sec. 2.2). It is therefore necessary to assess whether our ray design enhances, rather than hinders, the overall interaction experience.

Accordingly, we adapted a weight discrimination task from the literature, which required participants to judge the weight of two visually identical cups. The weights of the cups varied across conditions, allowing us to answer **RQ1** by examining whether RayFlex is sufficient for conveying weight sensations in VR. For **RQ2**, we compared our dynamic ray deformation with the commonly used straight ray, using the same displacement mechanism in both conditions to ensure that any differences could be attributed to the ray design itself.

4.1 Participants and Apparatus

A total of 20 participants (10 female, 10 male; 20–28 years, $M = 27.68$, $SD = 2.95$) participated in the study, with a sample size comparable to or larger than those used in previous pseudo-haptic studies [39, 47]. All participants had either normal or corrected-to-normal vision and reported no known motor or neurological disorders. To assess participants' familiarity with the VR system, we employed a 7-point Likert scale (1 = no prior experience, 7 = highly experienced). The mean rating was $M = 5.64$ ($SD = 1.73$). Our institutional ethics committee approved all procedures (Protocol No. HKUST(GZ)-HSP-2025-0049), and written informed consent was obtained before the study began.

The study was conducted using a Meta Quest 3 headset connected via a USB-C 3.2 cable to a laptop equipped with an Intel Core i9-13980HX processor, 64 GB DDR5 RAM, and an NVIDIA GeForce RTX 4070 GPU. Participants interacted with the virtual environment using the standard Quest controllers. The VR application was developed using Unity (version 2022.3.51f1) and ran on the connected laptop. All interaction events and data were automatically logged by the program for subsequent analysis.

4.2 Task

Participants performed a *two-alternative forced choice* (2AFC) task [32, 33], comparing the perceived weights of two visually identical cups (see Fig. 2). Each trial presented one cup with a fixed reference weight of 0.2 and another with a comparison weight based on the current experimental condition. The reference and comparison weights were randomly assigned to the two cups in each trial. Weight judgments were based solely on the experience of lifting each cup from the ground to a table positioned five Unity meters ahead. After placing both cups on the table, participants rearranged them, positioning the lighter cup on the left and the heavier one on the right. When satisfied, they confirmed their choice by pressing the X button on the left controller, after which the program recorded their response and proceeded to the next trial.

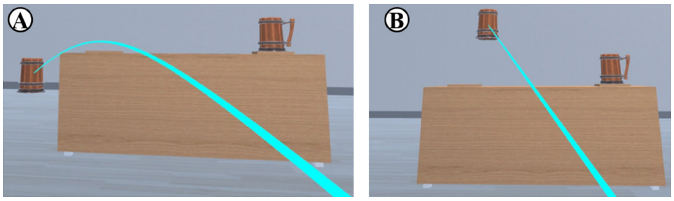

Fig. 2: The experimental scenario in Study 1, where participants lifted a virtual cup from the ground to the table. (A) RayFlex condition with dynamic ray deformation. (B) Straight ray condition with an undeformed ray.

To promote immersion and create a convincing interaction, participants were told that the cups contained different amounts of water to imply weight differences. However, no visual representation of the liquid was shown, ensuring that only the visual cues introduced by the tested technique influenced weight perception. To eliminate additional cues related to gravity or inertia, the placement interaction followed a rule with only two possible outcomes: a cup would remain on the table only if it were successfully placed on the surface, regardless of whether the participant's weight estimation was correct. Otherwise, it would instantly snap back to the ground without any transitional animation [32].

4.3 Experimental Design

This study employed a 2×10 within-subjects design with two independent variables: Ray Visualization (RV), comprising two levels (a dynamic ray deformation as designed in RayFlex and a conventional straight ray), and Object Mass (OM), with ten levels ranging from 0.4 to 2.2 in increments of 0.2. This resulted in a total of 20 experimental conditions.

In all experimental conditions, object movement was governed by our displacement mechanism (see Sec. 3.2). When combined with a dynamically deforming ray, this constitutes our proposed technique, RayFlex. To simplify terminology, we refer to RayFlex as the condition where ray deformation is applied throughout the remainder of this study. In comparison, the straight ray condition serves as a baseline representative of the ray commonly used in VR, where a straight ray continuously extends from the controller to the selected object (see Fig. 2).

To ensure a controlled comparison across conditions, we maintained consistent displacement model parameters throughout the study. Specifically, spring stiffness ($k = 20$ N/m) and damping ratio ($\zeta = 0.9$) were held constant in all conditions, while the ray scaling factor ($s = 0.5$) was applied only in the RayFlex condition (see Eq. (8)). These empirically determined values ensured stable, smooth, and perceptually meaningful motion across varying mass levels, non-oscillatory, and visually plausible. Note that these parameters are context-dependent and may be adjusted based on application-specific constraints.

The experiment was organized into two blocks, each corresponding to a distinct Ray Visualization. Within each block, participants completed trials involving ten different Object Mass levels. The order of blocks was counterbalanced across participants, and the presentation order of trials (1 OM × 1 repetition) within each block was randomized. Each condition (1 RV × 1 OM) was repeated twice per participant. In total, the study yielded 2 RV × 10 OM × 2 repetitions × 20 participants = 800 trials.

4.4 Procedure

Throughout the study, the experiment was conducted following a structured procedure. Participants were first welcomed to the study and asked to complete a pre-experiment questionnaire to collect demographic information. They were then introduced to the experimental task and assisted with wearing the VR headset. After a brief explanation of the task objectives and device usage, participants familiarized themselves with the virtual environment and interaction method through a

Table 1: Subjective questionnaire items used to assess weight perception, user satisfaction, presence, and perceived workload. Items were rated on a 7-point Likert scale.

Category	Question
Weight	WQ1: It was easy to choose an object that felt heavier than the other in each trial. WQ2: I could perceive different levels of heaviness across trials (e.g., in one trial, an object felt very much heavier, but in another trial, an object felt only slightly heavier than the other).
Satisfaction	SQ1: I think this technique would support weight perception in virtual reality. SQ2: I want to use this technique again in virtual reality.
Presence	PQ1: My interactions in the virtual space were natural. PQ2: The virtual environment was responsive to my actions. PQ3: I felt confident in my interactions in the virtual space at the end of the study.

short practice session (about 5 minutes) using an object mass that was not included in the experimental conditions. At the end of each block, participants completed a subjective questionnaire to evaluate their experience with the corresponding ray condition. After finishing all trials, an unstructured interview was conducted to elicit additional feedback and impressions. The entire study session lasted approximately 30 minutes.

4.5 Measurements

Both objective and subjective measures were collected in this study. Objective data were obtained from participants' performance in the 2AFC task, which was used to assess their ability to discriminate between virtual masses. For each condition, we computed the proportion of trials in which participants correctly identified the heavier object. Subjective data were collected through post-experiment questionnaires. Ratings on a 7-point Likert scale were used to assess three dimensions, weight perception, satisfaction, and presence, adapted from prior work [13] (see Tab. 1), while perceived workload was measured using the Raw NASA-TLX [10]. Additionally, participants were further asked to rank the two ray visualization methods according to their preferences and to provide reasons for their choices at the end of the experiment.

4.6 Results

We first assessed the normality of the data using the Shapiro–Wilk test. As the objective measures violated the normality assumption, we applied the Aligned Rank Transformation (ART) [46] to the data. We then conducted repeated-measures ANOVA, corrected the degrees of freedom with Greenhouse-Geisser correction, and reported partial eta squared as effect sizes when appropriate. Post-hoc comparisons were adjusted using the Bonferroni method to reduce the likelihood of Type I error. For subjective measures, within-subject differences between the two RV conditions were analyzed using the two-sided non-parametric Wilcoxon signed-rank test with a significance level of $\alpha = .05$. Where applicable, effect sizes were reported using the rank-biserial correlation r, computed as $r = \frac{Z}{\sqrt{N}}$.

4.6.1 Mass Discrimination Accuracy

RM-ANOVA results showed a significant main effect of OBJECT MASS ($F_{9,761} = 3.83$, $p < .001$, $\eta_p^2 = .043$), with no significant effect of RAY VISUALIZATION or their interaction (see Fig. 3 (A)). Pairwise comparisons indicated that accuracy in OM= 0.4 was significantly lower than all other mass conditions ($p < .05$ when OM $= 0.6$, 1.0, and 1.4, and $p < .001$ for the remaining). Notably, although accuracy at OM $= 0.4$ was significantly lower than in other conditions, it still achieved a high discrimination accuracy ($M = 90\%$), and the median discrimination accuracy remained at 100% across all object mass conditions.

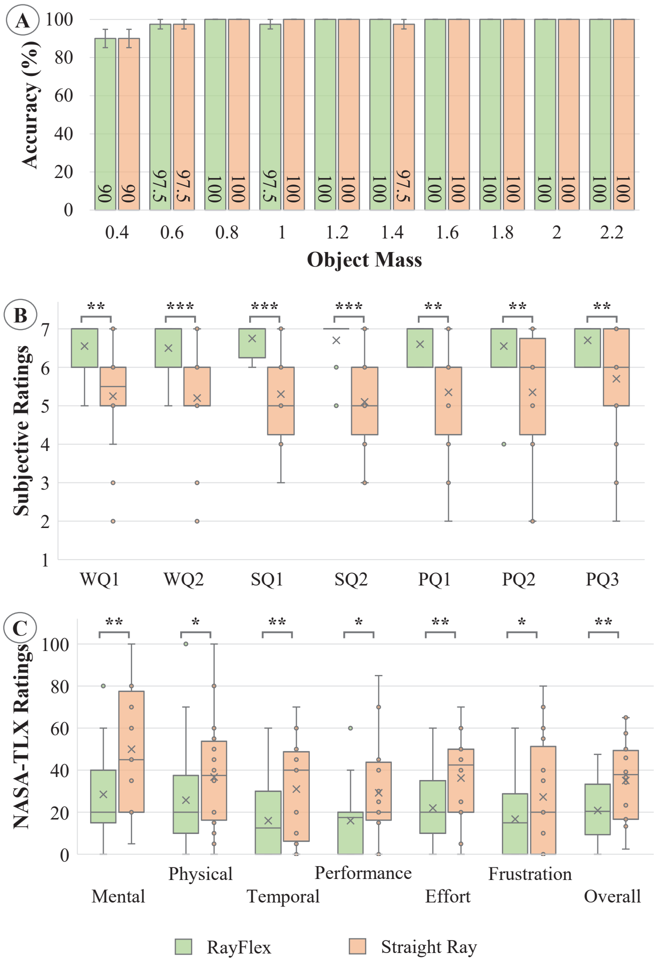

Fig. 3: Study 1 results. (A) Mass discrimination accuracy across object mass conditions. Error bars represent the standard error. (B) Subjective ratings on weight perception (WQ1–WQ2), satisfaction (SQ1–SQ2), and presence (PQ1–PQ3). (C) Raw NASA-TLX workload ratings. Lower ratings indicate lower workload. In (B) and (C), asterisks (*, **, ***) indicate significant differences at $p < .05$, $p < .01$, and $p < .001$, respectively.

4.6.2 Weight Perception

As illustrated in Fig. 3 (B), the Wilcoxon signed-rank test revealed that participants were able to reliably identify the heavier object in each trial (WQ1) and distinguish between different weight settings across the study (WQ2), regardless of the ray visualization. Across conditions, RayFlex received higher ratings than straight ray for both WQ1 (RayFlex: $Mdn = 7$, Straight: $Mdn = 5.5$) and WQ2 (RayFlex: $Mdn = 7$, Straight: $Mdn = 5$), with statistically significant differences on both WQ1 ($Z = 3.16$, $p = .002$, $r = .707$) and WQ2 ($Z = 3.30$, $p < .001$, $r = .739$).

4.6.3 Satisfaction

A similar pattern can be observed in users' satisfaction ratings (see Fig. 3 (B)). On both satisfaction questions, participants favored RayFlex over the straight ray. For SQ1, RayFlex received a higher rating ($Mdn = 7$) compared to straight ray ($Mdn = 5$), with a significant difference confirmed by the Wilcoxon signed-rank test ($Z = 3.33$, $p < .001$, $r = .744$). For SQ2, RayFlex was again rated higher ($Mdn = 7$) than the straight ray ($Mdn = 5$), with a statistically significant result ($Z = 3.43$, $p < .001$, $r = .766$).

4.6.4 Presence

Consistent with the previous findings, participants also reported stronger feelings of presence when using RayFlex (see Fig. 3 (B)).

For PQ1, which assessed the naturalness of interaction, RayFlex was rated notably higher than straight ray ($Mdn = 7$ vs. $Mdn = 6$; $Z = 3.06$, $p = .002$, $r = .685$). PQ2, measuring the responsiveness of the virtual environment, showed a similar pattern, with RayFlex again outperforming straight ray ($Mdn = 7$ vs. $Mdn = 6$; $Z = 3.08$, $p = .002$, $r = .688$). Finally, participants expressed greater confidence in their interactions by the end of the study (PQ3), as reflected by significantly higher ratings for RayFlex ($Mdn = 7$ vs. $Mdn = 6$; $Z = 2.76$, $p = .006$, $r = .617$).

4.6.5 Workload and Preferences Ranking

Participants reported lower perceived workload when interacting with RayFlex compared to the straight ray condition (see Fig. 3 (C)), with consistently better ratings across all NASA-TLX dimensions. Specifically, mental demand was rated significantly lower in the RayFlex condition ($Mdn = 20$) than in the straight ray condition ($Mdn = 45$; $Z = 2.65$, $p = .008$, $r = .592$). Similar patterns were observed for physical demand ($Mdn = 20$ vs. 37.5; $Z = 2.15$, $p = .031$, $r = .481$) and temporal demand ($Mdn = 12.5$ vs. 40; $Z = 3.13$, $p = .002$, $r = .700$). Performance ratings also favored RayFlex, indicating participants felt more successful with the interaction ($Mdn = 17.5$ vs. 20; $Z = 2.31$, $p = .021$, $r = .516$). In terms of effort and frustration, RayFlex was again perceived as superior. Ratings of effort required to complete the task were significantly lower ($Mdn = 20$ vs. 42.5; $Z = 2.71$, $p = .007$, $r = .606$), as were frustration scores ($Mdn = 15$ vs. 20; $Z = 2.56$, $p = .010$, $r = .573$). Overall workload also showed a significant reduction with RayFlex ($Mdn = 20.4$ vs. 37.9; $Z = 2.96$, $p = .003$, $r = .662$).

Finally, participants' overall preferences strongly favored RayFlex over straight ray. Among the 20 participants, 17 ranked RayFlex as their preferred interaction method, whereas only 3 preferred straight ray.

4.7 Discussion

4.7.1 Weight Perception (RQ1)

In terms of weight perception, no significant differences were observed between the two RAY VISUALIZATION concerning weight discrimination accuracy (see Sec. 4.6.1). A significant main effect was found only for OBJECT MASS, where the 0.4 mass condition yielded the lowest accuracy. However, even in this condition, performance remained at 90%, indicating that participants could generally distinguish weight levels reliably. Furthermore, a clear trend emerged, with accuracy improving as object weight increased. These results suggest that participants were able to effectively infer an object's mass regardless of the ray used. We attribute this to the effectiveness of our displacement mechanism, which conveyed weight through observable spatial lag and temporal delay. Participants' qualitative feedback further supports this. As P6 noted, "*I enjoy dragging the cup to judge its weight from the movement and delay.*"

Notably, although no significant differences in task performance were observed, we posit that the dynamic ray deformation nonetheless complemented the displacement mechanism by guiding users' visual attention and reinforcing the perception of object weight. This interpretation is substantiated by responses to WQ1 and WQ2 (see Sec. 4.6.2), where RayFlex received significantly higher ratings for supporting the perception of heaviness, compared to the conventional straight ray condition. Several participants highlighted that the deformation of the ray offered more immediate and intuitive visual cues for estimating object weight. As P18 remarked, distinguishing weight using the straight ray required deliberate attention: "*I can tell the difference in weight if it's straight, but only if I pay close attention. It's not like RayFlex, where you can rely on the deformation.*" Echoing this, P8 noted, "*I can quickly judge the weight by the fluctuation of the curve when there is a big difference.*"

Therefore, in response to **RQ1**, we conclude that participants were able to reliably discriminate object weights based on the displacement mechanism, regardless of the ray visualization method. The dynamic ray deformation in RayFlex acted as a complementary cue, providing additional visual support during weight estimation.

4.7.2 Ray Deformation (RQ2)

To ensure that the proposed dynamic ray deformation did not introduce unnecessary visual distraction or compromise user experience due to increased visual complexity, we evaluated it across several dimensions. First, regarding user satisfaction, most participants reported that RayFlex offered a more favorable experience than the straight ray, particularly in conveying weight sensations (SQ1). Furthermore, the majority expressed a willingness to use RayFlex again in future VR systems (SQ2).

Second, regarding presence, RayFlex was perceived to provide a more natural (PQ1), intuitive (PQ2), and immersive experience (PQ3) than the straight ray condition. This outcome can be attributed to the design of RayFlex, which draws an analogy to real-world physical behavior, thereby enhancing users' sense of presence and allowing them to relate the interaction more closely to their daily experiences.

Finally, in terms of workload, RayFlex received consistently lower ratings across all NASA-TLX dimensions. As discussed in Sec. 4.7.1, the reduction in mental demand can be attributed to the ray deformation providing complementary visual cues for weight inference, thereby reducing reliance on displacement-based cues alone. This visual cue also reduced physical demand by minimizing the need for repeated lifting or adjustment actions. In addition, participants reported lower temporal pressure, as the ray enabled faster judgments without being constrained by timing demands. The increased clarity of visual cues may have further contributed to higher performance and less frustration. As a result, the overall workload associated with RayFlex was also consistently lower.

In summary, the results indicate that our ray design did not introduce cognitive or perceptual burden, such as visual distraction or increased task demand. Instead, it served as a beneficial visual augmentation that enhanced users' ability to perceive object weight and enriched the overall interaction experience. Therefore, in response to **RQ2**, we conclude that the dynamic ray deformation, when combined with our displacement mechanism, constitutes a reasonable and effective design for supporting pseudo-haptic weight perception while maintaining clarity, usability, and immersion.

5 STUDY 2: EVALUATING SUBJECTIVE EXPERIENCE WITH RAYFLEX IN APPLICATION CONTEXTS

Building on the validated effectiveness of RayFlex, we further assessed its user experience compared to conventional raycasting, a widely adopted technique in modern VR systems, to answer the following research question.

RQ3. How does RayFlex influence users' subjective experience? Previous work has not incorporated weight perception into raycasting-based interaction, leaving its impact on user experience largely unexplored. Thus, it is essential to examine users' subjective responses in this context to understand how the weight sensation impacts their experience and to inform the design of future raycasting-based interaction techniques.

Correspondingly, we designed two task-oriented VR games involving distinct interaction scenarios. In both tasks, RayFlex was compared against conventional raycasting, where a straight ray is projected from the controller to the target, and the selected object is rigidly attached to the ray tip. This design results in a direct and immediate mapping between user input and object behavior, fundamentally differing from RayFlex. The rationale for including this comparison and the two task designs was based on two key considerations. First, to the best of our knowledge, no prior work has examined the integration of pseudo-haptic cues to support weight perception in raycasting-based interaction. Second, user preferences may vary across task contexts, as each technique may provide distinct advantages depending on the nature of the interaction.

5.1 Participants and Apparatus

Consistent with Study 1, this study included 20 participants (7 female, 13 male), aged 19 to 26 years ($M = 22.36$, $SD = 2.12$). All met the same eligibility requirements and followed the same recruitment, screening,

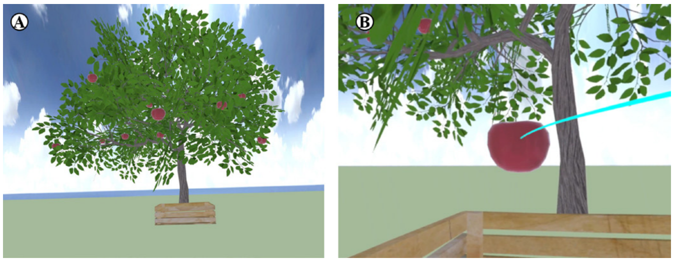

Fig. 4: Experimental scenarios in Study 2, Task 1. (A) Harvest Drop simulates lightweight object interaction, where participants pick and deposit apples (highlighted in red) using ray-based techniques. (B) A user is putting an apple into the basket.

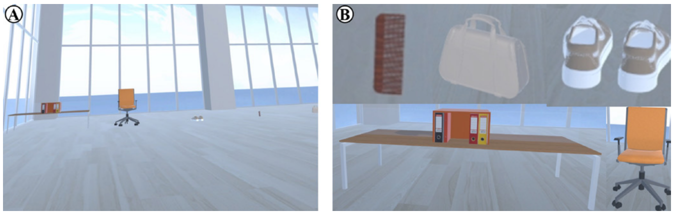

Fig. 5: Experimental scenarios in Study 2, Task 2. (A) Tidy Quest requires relocating five scattered virtual objects of varying masses to their designated positions within a room. (B) The five objects used in the study: a comb, a bag, shoes, a table, and a chair.

and consent procedures as in Study 1. Prior VR experience was again rated on a 7-point Likert scale, with an average score of $M = 3.65$ ($SD = 1.72$). The same apparatus was utilized as in Study 1, too.

5.2 Tasks

5.2.1 Task 1: Harvest Drop

The purpose of this task was to simulate everyday interactions involving lightweight objects. Participants stood in front of a virtual apple tree with a basket placed beneath it (see Fig. 4 (A)). Using the ray-based interaction technique, they were instructed to pick apples from the tree and deposit them into the basket (see Fig. 4 (B)). Each tree contained ten apples that varied in appearance, size, and virtual mass (mass ranging from 0.05 to 0.32, in increments of 0.03). The task was completed once all ten apples were successfully placed into the basket. To ensure completion, any apple released outside the basket was automatically returned to its original position on the tree, requiring the participant to repeat the action.

5.2.2 Task 2: Tidy Quest

This task was designed to replicate interaction scenarios involving heavy objects and noticeable differences in virtual mass. Participants were instructed to perform a virtual clean-up activity, in which scattered objects had to be returned to their designated locations within a virtual room (see Fig. 5 (A)). Target locations were visually indicated by semi-transparent placeholders. Five objects were used: a table, a chair, a bag, a pair of shoes, and a comb, with virtual masses of 10, 6, 3, 0.5, and 0.1, respectively (see Fig. 5 (B)). All objects were initially placed randomly, approximately 5 meters from the participant's starting position. To maintain realism, collision detection was implemented to prevent objects from penetrating the floor, including under vertical displacements induced by RayFlex. The task was considered complete once all objects were accurately returned to their corresponding placeholders.

5.3 Technique Specification and Experimental Design

In this study, two techniques were employed: RayFlex and conventional raycasting. To accommodate the interaction demands of each task, RayFlex parameters were adjusted accordingly. In the Harvest Drop, the spring stiffness was reduced to $k = 5$ N/m while the damping ratio remained at $\zeta = 0.9$, to emphasize the sensation of gravitational pull when grasping an apple. This configuration produced a subtle downward displacement upon contact, reinforcing the intended weight illusion. In contrast, the Tidy Quest adopted the same configuration as in Study 1 ($k = 20$ N/m, $\zeta = 0.9$), ensuring precise control and stable motion during manipulation. The ray scaling factor was held constant across tasks at $s = 0.5$.

The experiment proceeded using a procedure similar to that of Study 1. Participants first completed a demographic questionnaire and were given a brief explanation of the study purpose. They then engaged in a three-minute practice session for each task to familiarize themselves with the interaction techniques and environment mechanics. The formal session consisted of two blocks, each corresponding to one task. Within each block, participants performed the task using both techniques in a counterbalanced order. They were instructed to complete the tasks at their own pace, without any time constraints. After each technique, participants completed a set of subjective questionnaires to assess their experience. Upon completing both blocks, they indicated their preferred technique for each task. The session concluded with a short interview to collect open-ended feedback.

Unlike Study 1, which focused on evaluating the rationale and effectiveness of individual design components, this second study aimed to investigate users' subjective experience and preferences toward the overall technique across different contexts. To this end, four standardized questionnaires were employed to assess user experience along four dimensions: workload (Raw NASA Task Load Index, NASA-TLX [10]), usability (System Usability Scale, SUS [23]), user experience (short version of the User Experience Questionnaire, UEQ-S [34]), and presence (Slater-Usoh-Steed Presence Questionnaire, SUSQ [40]).

5.4 Results

5.4.1 Harvest Drop

The same analysis methods as in Study 1 were applied, and only statistically significant results are reported in this section. NASA-TLX results revealed that participants experienced significantly higher subjective workload with RayFlex compared to the baseline (see Fig. 6 (A)). Specifically, mental demand was substantially greater with RayFlex ($Mdn = 20$) than with the typical raycasting technique ($Mdn = 20$; $Z = 2.11$, $p = .035$, $r = .472$). Similar effects were found for physical demand ($Mdn = 32.5$ vs. 15; $Z = 3.04$, $p = .002$, $r = .681$) and temporal demand ($Mdn = 37.5$ vs. 17.5; $Z = 2.77$, $p = .006$, $r = .62$), both showing increases under RayFlex. Participants also reported higher effort with RayFlex ($Mdn = 25$ vs. 12.5; $Z = 2.65$, $p = .008$, $r = .593$). Overall workload was likewise judged to be significantly more demanding in the RayFlex ($Mdn = 32.1$ vs. 14.6; $Z = 2.72$, $p = .007$, $r = .607$).

Beyond workload, perceived usability was assessed using the System Usability Scale (see Fig. 6 (B)). RayFlex demonstrated superior usability, with users assigning it higher scores ($Mdn = 78.75$) than the baseline ($Mdn = 66.25$; $Z = 2.34$, $p = .019$, $r = .523$).

For a broader view of user experience, we examined results from the UEQ-S (see Fig. 6 (C)). RayFlex was consistently rated more favorably across both dimensions. In terms of pragmatic quality, it received significantly higher ratings ($Mdn = 2.25$ vs. $Mdn = 1.25$; $Z = 3.49$, $p < .001$, $r = .779$), indicating greater perceived efficiency and functionality. Regarding hedonic quality, RayFlex was also favored, with notably more positive impressions ($Mdn = 2.5$ vs. $Mdn = -1.125$; $Z = 3.91$, $p < .001$, $r = .874$), reflecting stronger enjoyment and engagement. The overall user experience score further confirmed this trend ($Mdn = 2.38$ vs. $Mdn = -0.25$; $Z = 3.9$, $p < .001$, $r = .873$). This advantage in overall user experience was also reflected in the user preference ranking, where 90% of participants indicated a preference for RayFlex (see Fig. 6 (H)); two-sided binomial test, $p < .001$).

Finally, participants reported a stronger sense of presence when using RayFlex (see Fig. 6 (D)). The presence score was higher with RayFlex ($Mdn = 5.83$) compared to the traditional ray ($Mdn = 3$), representing a large effect size ($Z = 3.90$, $p < .001$, $r = .873$).

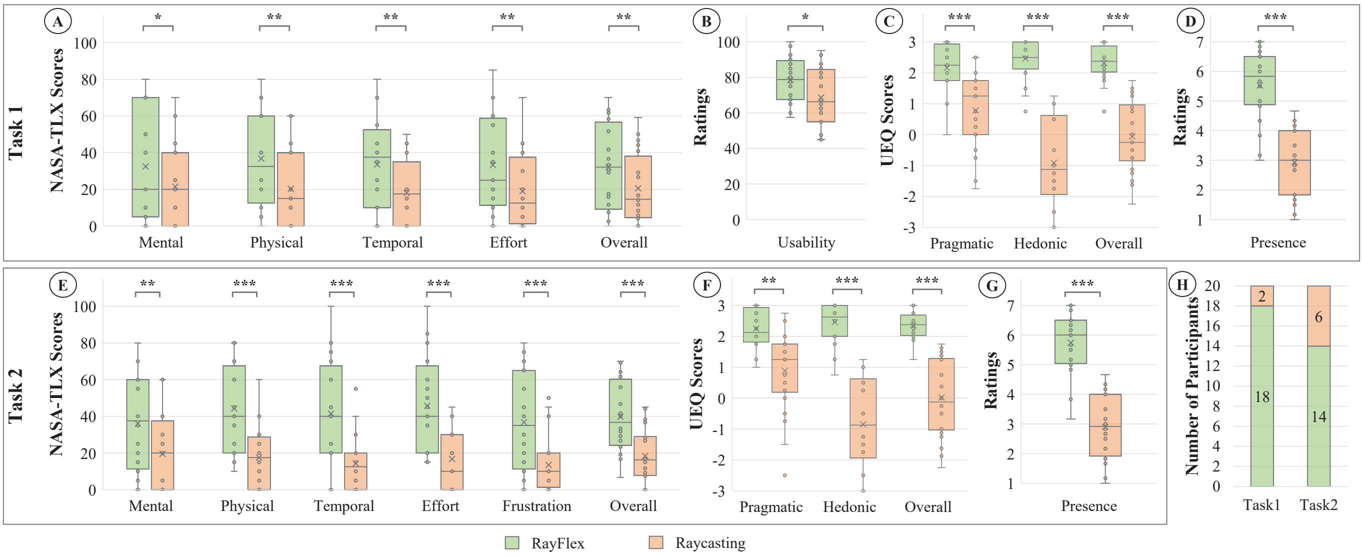

Fig. 6: Study 2 results across the two VR interaction tasks: Harvest Drop (top row, Panels A–D) and Tidy Quest (bottom row, Panels E–G). Error bars represent the standard error of the mean. Asterisks indicate significance levels (* $p < .05$, ** $p < .01$, *** $p < .001$). (A, E) NASA-TLX workload ratings across six dimensions and overall workload. (B) System Usability Scale scores. (C, F) UEQ scores. (D, G) Presence ratings. (G) Participant preferences between RayFlex and raycasting for each task. (H) Users' preferences ranking

5.4.2 Tidy Quest

In the Tidy Quest task, participants again reported significantly greater workload when using RayFlex compared to the baseline raycasting (see Fig. 6 (E)). Mental demand was notably higher for RayFlex ($Mdn = 37.5$ vs. $Mdn = 20$; $Z = 3.07$, $p = .002$, $r = .687$), along with physical demand ($Mdn = 40$ vs. $Mdn = 17.5$; $Z = 3.88$, $p < .001$, $r = .868$) and temporal demand ($Mdn = 40$ vs. $Mdn = 12.5$; $Z = 3.71$, $p < .001$, $r = .829$). Effort ratings also reflected a substantial increase for RayFlex ($Mdn = 40$ vs. $Mdn = 10$; $Z = 3.88$, $p < .001$, $r = .867$), as did frustration levels ($Mdn = 35$ vs. $Mdn = 10$; $Z = 3.38$, $p < .001$, $r = .757$). The overall workload score followed this pattern, with RayFlex perceived as significantly more demanding overall ($Mdn = 36.67$ vs. $Mdn = 16.25$; $Z = 3.87$, $p < .001$, $r = .864$).

Regarding user experience, RayFlex demonstrates a clear advantage (see Fig. 6 (F)). Pragmatic quality favored RayFlex, with higher ratings for perceived effectiveness and functionality ($Mdn = 2.13$ vs. $Mdn = 1.25$; $Z = 3.2$, $p = .001$, $r = .715$). Hedonic quality ratings were also more positive ($Mdn = 2.63$ vs. $Mdn = -0.88$; $Z = 3.91$, $p < .001$, $r = .874$), highlighting enhanced engagement and enjoyment. The overall UEQ-S score further confirmed this preference ($Mdn = 2.38$ vs. $Mdn = -0.13$; $Z = 3.90$, $p < .001$, $r = .873$). This pattern was also reflected in participants' preference rankings, where 70% (14/20) preferred RayFlex to the baseline (see Fig. 6 (H); two-sided binomial test, $p = .115$).

Presence ratings showed a similar pattern (see Fig. 6 (G)). Participants reported a stronger sense of immersion with RayFlex ($Mdn = 6$) compared to the conventional ray ($Mdn = 2.92$), supported by a large effect ($Z = 3.90$, $p < .001$, $r = .873$).

5.5 Discussion: RayFlex in Applications (RQ3)

Results showed that RayFlex consistently induced a higher perceived workload than the baseline across two tasks. This observation is consistent with prior research [29], which reported increased workload associated with implementing pseudo-haptic feedback. Additionally, a positive association was observed between the perceived heaviness of virtual objects and participants' reported workload. This was evident in Tidy Quest (Task 2), which several participants (e.g., P1, P5, P13, P19) described as more demanding than Harvest Drop (Task 1), primarily due to the increased effort required to manipulate heavier virtual items such as a table and a chair.

Despite the elevated workload, RayFlex demonstrated advantages in other aspects of subjective experience. In terms of usability and preference rankings, it significantly outperformed the baseline in Harvest Drop. However, this advantage did not extend to Tidy Quest, where no significant difference between techniques was observed. One possible explanation is that the increased workload associated with handling heavier objects may have attenuated the perceived usability benefits of RayFlex, leading to comparable ratings for both techniques. Participants' qualitative feedback supports this interpretation. For instance, P13 noted that while RayFlex felt "more realistic," completing the task remained "quite exhausting" due to the excessive object's weight. In contrast, although the baseline lacked weight simulation, it was perceived as more efficient for completing the task.

Notably, participants did not uniformly interpret the increased workload as a drawback. Several described the additional demand as "expected" or "natural" when simulating handling heavy objects. As P20 remarked, "*It felt harder, but in a good way; it made me more careful, like I was lifting something.*" This suggests that higher workload, when aligned with the task context and perceptual realism, may not necessarily diminish user experience. Consistent with this interpretation, broader user experience measures favored RayFlex. UEQ-S ratings revealed higher scores on both pragmatic and hedonic dimensions, with all values exceeding the "excellent" performance benchmark. Participants described RayFlex as not only functionally effective but also more engaging and enjoyable to use. As P7 noted, "*With RayFlex, I felt more connected to the object. It wasn't just pointing and drawing; it felt like real interaction.*" This increased engagement was further reflected in presence ratings, which were significantly higher for RayFlex, with participants reporting stronger immersion and presence across both tasks.

In response to **RQ3**, the findings indicate that although RayFlex increased perceived workload, participants often regarded this as natural and contextually appropriate. As a result, RayFlex led to improvements in usability (in Task 1), as well as enhanced engagement and presence, with participants reporting a more immersive and realistic experience.

6 Design Implications and Application Guidelines

Based on the findings from two user studies, we present two design implications (**DI#**) to inform future development of raycasting-based pseudo-haptic techniques, along with an application guideline (**AG#**) to support the practical implementation of RayFlex in VR systems.

DI1 *Leverage ray–object decoupling to enable richer pseudo-haptic* *effects.* Raycasting offers structural separation between the ray's visual representation and the object's response. This decoupling enables designers to independently design ray appearance and object dynamics, allowing pseudo-haptic cues to be adapted to the interaction context without compromising spatial coherence or user embodiment.

DI2 *Calibrate virtual weight to balance realism and interaction efficiency.* Simulating object weight can enhance realism and support task engagement. However, assigning overly high mass may lead to increased workload and reduced usability. These findings highlight the importance of calibrating virtual weight according to task demands, while avoiding values that impose unnecessary strain on users.

AG1 *Tune RayFlex parameters to support diverse interaction goals.* RayFlex exposes a set of configurable parameters, including spring stiffness (k), damping ratio (ζ), and curvature scaling (s), that can be adjusted to match different interaction demands. Designers can configure these parameters based on specific application scenarios to achieve the desired pseudo-haptic behavior.

7 Conclusion, Limitations, and Future Work

This work presented RayFlex, a pseudo-haptic technique that enables weight sensation in raycasting-based VR interaction. By combining a mass-spring-damper model with dynamic ray deformation, RayFlex simulates object heaviness without physical feedback. Two user studies confirmed its effectiveness in both controlled and application-oriented settings, showing improved weight discrimination, user satisfaction, and presence.

While RayFlex successfully supports visual weight perception in ray-based interaction, several limitations remain. First, the technique relies solely on visual cues, which may not generalize well to users with limited visual sensitivity or in visually complex environments. Future work will investigate hybrid feedback approaches that combine pseudo-haptics with lightweight tactile or auditory cues to address this limitation. Second, the current evaluation focused on assessing the effectiveness of the technique in eliciting weight perception rather than explicitly quantifying perceptual thresholds. As such, psychophysical methods such as Just-Noticeable Difference (JND) measurements and psychometric curve fitting were not employed. While this approach was sufficient for establishing the presence and relative strength of the effect, future work could adopt JND-based paradigms to more precisely characterize users' sensitivity to weight changes and provide a finer-grained understanding of the perceptual response induced by RayFlex. Third, the mass-spring-damper parameters were fixed across tasks and participants. Personalized or adaptive parameter tuning may enhance both perceptual realism and interaction comfort. To this end, we plan to explore automatic adaptation strategies based on user behavior or task context. Finally, our evaluation focused on isolated object lifting tasks. Future research could examine the applicability of RayFlex in broader interaction contexts, such as multi-object manipulation, cooperative tasks, or bare-hand interaction, as well as the potential influence of controller weight on weight assessment, to further assess its generalizability across tasks and interaction modalities.

Acknowledgements

The authors thank our participants for their time and the reviewers for their comments and suggestions, which helped improve our paper. This work is supported in part by the National Key Research and Development Program of China (Grant № 2024YFC3307602), the Guangdong Provincial Talent Program (Grant № 2023JC10X009), the Guangzhou Development Zone Science and Technology Project (Grant № 2023GH02), and the Science and Technology Development Funds of Macau (Grant № 0019/2025/RIB1).

References

[1] A. Achberger. Stroe: An ungrounded string-based weight simulation device. In *Proceedings of the 2022 IEEE Conference on Virtual Reality and 3D User Interfaces (VR)*, pp. 112–120. IEEE, New Zealand (Virtual), 2022. doi: 10.1109/VR51125.2022.00029 2

[2] N. Ahmed, M. Lataifeh, and I. N. Junejo. Visual pseudo haptics for a dynamic squeeze / grab gesture in immersive virtual reality. *2021 IEEE 2nd International Conference on Human-Machine Systems (ICHMS)*, pp. 1–4, 2021. doi: 10.1109/ICHMS53169.2021.9582654 2

[3] F. Argelaguet and C. Andujar. Special section on touching the 3rd dimension: A survey of 3d object selection techniques for virtual environments. *Comput. Graph.*, 37(3):121–136, 16 pages, May 2013. doi: 10.1016/j.cag.2012.12.003 2

[4] M. Baloup, T. Pietrzak, and G. Casiez. Raycursor: A 3d pointing facilitation technique based on raycasting. In *Proceedings of the 2019 CHI Conference on Human Factors in Computing Systems*, CHI '19, 12 pages, p. 1–12. Association for Computing Machinery, New York, NY, USA, 2019. doi: 10.1145/3290605.3300331 2

[5] D. L. Chen, M. Giordano, H. Benko, T. Grossman, and S. Santosa. Gazeraycursor: Facilitating virtual reality target selection by blending gaze and controller raycasting. In *Proceedings of the 29th ACM Symposium on Virtual Reality Software and Technology (VRST '23)*, 2023. doi: 10.1145/3611659.3615693 2

[6] I. Choi, H. Culbertson, M. R. Miller, A. Olwal, and S. Follmer. Grabity: A wearable haptic interface for simulating weight and grasping in virtual reality. In *Proceedings of the 30th Annual ACM Symposium on User Interface Software and Technology (UIST '17)*, pp. 119–130. Association for Computing Machinery, New York, NY, USA, 2017. doi: 10.1145/3126594.3126599 2

[7] K. Collins and B. Kapralos. Pseudo-haptics: leveraging cross-modal perception in virtual environments. *The Senses and Society*, 14:313 – 329, 2019. doi: 10.1080/17458927.2019.1619318 2

[8] A. Costes, F. Argelaguet, F. Danieau, P. Guillotel, and A. Lécuyer. Touchy: a visual approach for simulating haptic effects on touchscreens. *Frontiers in ICT*, 6:1, 2019. 2

[9] L. Dominjon, A. Lecuyer, J.-M. Burkhardt, P. Richard, and S. Richir. Influence of control/display ratio on the perception of mass of manipulated objects in virtual environments. In *IEEE Proceedings. VR 2005. Virtual Reality, 2005.*, pp. 19–25, 2005. doi: 10.1109/VR.2005.1492749 2

[10] S. G. Hart. Nasa-task load index (nasa-tlx); 20 years later. In *Proceedings of the human factors and ergonomics society annual meeting*, vol. 50, pp. 904–908. Sage publications Sage CA: Los Angeles, CA, 2006. 5, 7

[11] J. D. Hincapié-Ramos, K. Özacar, P. Irani, and Y. Kitamura. Gyrowand: Imu-based raycasting for augmented reality head-mounted displays. *Proceedings of the 3rd ACM Symposium on Spatial User Interaction*, 2015. doi: 10.1145/2788940.2788947 2

[12] Y.-M. Huang, T.-W. Mi, and L. Chan. Preview teleport: An occlusion-free point-and-teleport technique enhanced with an augmented preview. *IEEE Transactions on Visualization and Computer Graphics*, 31(5):2546–2556, 2025. doi: 10.1109/TVCG.2025.3549138 2

[13] C. Hwang, T. Feuchtner, and K. Grønbæk. Pseudo-haptics for weight perception in vr: Controller vs. bare hand interactions with tracking delay and vertical offset. In *2024 10th International Conference on Virtual Reality, ICVR 2024*, pp. 91–99, 2025. 10th International Conference on Virtual Reality ; Conference date: 24-07-2024 Through 26-07-2024. doi: 10.1109/ICVR62393.2024.10868891 1, 2, 5

[14] P. Issartel, F. Guéniat, S. Coquillart, and M. Ammi. Perceiving mass in mixed reality through pseudo-haptic rendering of newton's third law. In *2015 IEEE Virtual Reality (VR)*, pp. 41–46, 2015. doi: 10.1109/VR.2015.7223322 2

[15] A. Kalus, M. Kocur, J. Klein, M. Mayer, and N. Henze. Pumpvr: Rendering the weight of objects and avatars through liquid mass transfer in virtual reality. In *Proceedings of the 2023 CHI Conference on Human Factors in Computing Systems (CHI '23)*, article no. 263, pp. 1–13. Association for Computing Machinery, New York, NY, USA, 2023. doi: 10.1145/3544548.3581172 2

[16] D. Kharlamov, K. Pietroszek, and L. Tahai. Ticktockray demo: Smartwatch raycasting for mobile hmds. *Proceedings of the 2016 Symposium on Spatial User Interaction*, 2016. doi: 10.1145/2983310.2989206 1, 2

[17] J. Kim, S. Kim, and J. Lee. The effect of multisensory pseudo-haptic feedback on perception of virtual weight. *IEEE Access*, 10:5129–5140, 2022. doi: 10.1109/ACCESS.2022.3140438 2

[18] J. Kim and J. Lee. The effect of the virtual object size on weight perception augmented with pseudo-haptic feedback. *2021 IEEE Conference on Virtual Reality and 3D User Interfaces Abstracts and Workshops (VRW)*, pp. 575–576, 2021. doi: 10.1109/VRW52623.2021.00170 2

[19] M. Kim, J. Kim, K. Jeong, and C.-H. Kim. Grasping vr: Presence of pseudo-haptic interface based portable hand grip system in immersive virtual reality. *International Journal of Human–Computer Interaction*, 36:685 – 698, 2019. doi: 10.1080/10447318.2019.1680920 1, 2

[20] W. Kim, J. Jung, and S. Xiong. Vrmouse: Mouse emulation with the vr controller for 2d selection in vr. In T. Ahram and C. Falcão, eds., *Advances in Usability, User Experience, Wearable and Assistive Technology*, vol. 1217 of *Advances in Intelligent Systems and Computing*, pp. 663–670. Springer, Cham, 2020. doi: 10.1007/978-3-030-51828-8_87 2

[21] A. Kumar, R. Gourishetti, and M. Manivannan. Mechanics of pseudo-haptics with computer mouse. In *2017 IEEE International Symposium on Haptic, Audio and Visual Environments and Games (HAVE)*, 6 pages, p. 1–6. IEEE Press, 2017. doi: 10.1109/HAVE.2017.8240358 2

[22] A. Lecuyer, S. Coquillart, A. Kheddar, P. Richard, and P. Coiffet. Pseudo-haptic feedback: can isometric input devices simulate force feedback? In *Proceedings IEEE Virtual Reality 2000 (Cat. No.00CB37048)*, pp. 83–90, 2000. doi: 10.1109/VR.2000.840369 2

[23] J. R. Lewis. The system usability scale: Past, present, and future. *International Journal of Human–Computer Interaction*, 34(7):577–590, 2018. doi: 10.1080/10447318.2018.1455307 7

[24] Y. Li, F. Lu, W. Lages, and D. Bowman. Gaze direction visualization techniques for collaborative wide-area model-free augmented reality. *Symposium on Spatial User Interaction*, 2019. doi: 10.1145/3357251.3357583 2

[25] S. Lontschar, D. Deegan, I. Humer, K. Pietroszek, and C. Eckhardt. Analysis of haptic feedback and its influences in virtual reality learning environments. In *2020 6th International Conference of the Immersive Learning Research Network (iLRN)*, pp. 171–177. IEEE, 2020. doi: 10.23919/ilrn47897.2020.9155087 2

[26] T. Luong, Y. F. Cheng, M. Möbus, A. Fender, and C. Holz. Controllers or bare hands? a controlled evaluation of input techniques on interaction performance and exertion in virtual reality. *IEEE Transactions on Visualization and Computer Graphics*, 29(11):4633–4643, 2023. doi: 10.1109/TVCG.2023.3320211 1, 2

[27] X. Lv, C. Xue, and W. Xiao. Influence of size and depth perception on ray-casting interaction in virtual reality. In D. Russo, T. Ahram, W. Karwowski, G. D. Bucchianico, and R. Taiar, eds., *Intelligent Human Systems Integration 2021*, pp. 152–158. Springer International Publishing, Cham, 2021. 2

[28] D. Monteiro, H.-N. Liang, X. Wang, W. Xu, and H. Tu. Design and development of a low-cost device for weight and center of gravity simulation in virtual reality. In *Proceedings of the 2021 International Conference on Multimodal Interaction*, ICMI '21, 8 pages, p. 453–460, 2021. doi: 10.1145/3462244.3479907 1, 2

[29] M. S. Moosavi, P. Raimbaud, C. Guillet, J. Plouzeau, and F. Merienne. Weight perception analysis using pseudo-haptic feedback based on physical work evaluation. *Frontiers in Virtual Reality*, 4, 2023. doi: 10.3389/frvir.2023.973083 2, 8

[30] K. L. Palmerius, D. Johansson, G. Höst, and K. Schönborn. An analysis of the influence of a pseudo-haptic cue on the haptic perception of weight. In M. Auvray and C. Duriez, eds., *Haptics: Neuroscience, Devices, Modeling, and Applications. EuroHaptics 2014*, vol. 8618 of *Lecture Notes in Computer Science*, pp. 140–147. Springer, Berlin, Heidelberg, 2014. doi: 10.1007/978-3-662-44193-0_16 2

[31] S. J. Park, M. J. Kim, Y.-G. Son, D. Park, and Y. Lee. A comparative study on methods to interact with close-distance objects in mixed reality environment: Direct method vs. raycasting method. In *HCI International 2024 – Late Breaking Papers*, pp. 92–101. Springer, Cham, 2024. doi: 10.1007/978-3-031-61950-2_11 2

[32] M. Rietzler, F. Geiselhart, J. Gugenheimer, and E. Rukzio. Breaking the tracking: Enabling weight perception using perceivable tracking offsets. In *Proceedings of the 2018 CHI Conference on Human Factors in Computing Systems*, CHI '18, 12 pages, p. 1–12. Association for Computing Machinery, New York, NY, USA, 2018. doi: 10.1145/3173574.3173702 1, 2, 4

[33] M. Samad, E. Gatti, A. Hermes, H. Benko, and C. Parise. Pseudo-haptic weight: Changing the perceived weight of virtual objects by manipulating control-display ratio. In *Proceedings of the 2019 CHI Conference on Human Factors in Computing Systems*, CHI '19, 13 pages, p. 1–13. Association for Computing Machinery, New York, NY, USA, 2019. doi: 10.1145/3290605.3300550 1, 2, 4

[34] M. Schrepp, A. Hinderks, and J. Thomaschewski. Design and evaluation of a short version of the user experience questionnaire (UEQ-S). *International Journal of Interactive Multimedia and Artificial Intelligence*, 4(6):103–108, 2017. doi: 10.9781/ijimai.2017.09.001 7

[35] R. Shi, Y. Wei, X. Hu, Y. Liu, Y. Yue, L. Yu, and H.-N. Liang. Experimental analysis of freehand multi-object selection techniques in virtual reality head-mounted displays. *Proc. ACM Hum.-Comput. Interact.*, 8(ISS), article no. 529, 19 pages, Oct. 2024. doi: 10.1145/3698129 1

[36] J. Shigeyama, T. Hashimoto, S. Yoshida, T. Narumi, T. Tanikawa, and M. Hirose. Transcalibur: A weight shifting virtual reality controller for 2d shape rendering based on computational perception model. In *Proceedings of the 2019 CHI Conference on Human Factors in Computing Systems (CHI '19)*, pp. 1–11. Association for Computing Machinery, New York, NY, USA, 2019. doi: 10.1145/3290605.3300241 2

[37] C. Stellmacher, M. Bonfert, E. Kruijff, and J. Schöning. Triggermuscle: Exploring weight perception for virtual reality through adaptive trigger resistance in a haptic vr controller. *Frontiers in Virtual Reality*, 2:173, 2021. doi: 10.3389/frvir.2021.754511 2

[38] C. Stellmacher, F. I. Pujianto, T. Kojic, J.-N. Voigt-Antons, and J. Schöning. Experiencing dynamic weight changes in virtual reality through pseudo-haptics and vibrotactile feedback. In *Proceedings of the 2024 CHI Conference on Human Factors in Computing Systems*, CHI '24, article no. 421, 13 pages. Association for Computing Machinery, New York, NY, USA, 2024. doi: 10.1145/3613904.3642552 1, 2

[39] Y. Ujitoko and Y. Ban. Survey of pseudo-haptics: Haptic feedback design and application proposals. *IEEE Transactions on Haptics*, 14(4):699–711, 2021. doi: 10.1109/TOH.2021.3077619 1, 2, 4

[40] M. Usoh, E. Catena, S. Arman, and M. Slater. Using presence questionnaires in reality. *Presence: Teleoper. Virtual Environ.*, 9(5):497–503, 7 pages, Oct. 2000. doi: 10.1162/105474600566989 7

[41] V. Van Polanen, R. Tibold, A. Nuruki, and M. Davare. Visual delay affects force scaling and weight perception during object lifting in virtual reality. *Journal of Neurophysiology*, 121(4):1398–1409, Apr. 2019. doi: 10.1152/jn.00396.2018 2

[42] X. Wang, D. Monteiro, L.-H. Lee, P. Hui, and H.-N. Liang. Vibroweight: Simulating weight and center of gravity changes of objects in virtual reality for enhanced realism. In *2022 IEEE Haptics Symposium (HAPTICS)*, pp. 1–7, 2022. doi: 10.1109/HAPTICS52432.2022.9765609 1, 2

[43] J. Wei, K. Zhu, and Y. Ye. Fanray: Using fan mechanism in ray-casting to improve target selection in vr. *Proceedings of the 2023 3rd International Conference on Human Machine Interaction*, 2023. doi: 10.1145/3604383.3604395 2

[44] Y. Wei, R. Shi, D. Yu, Y. Wang, Y. Li, L. Yu, and H.-N. Liang. Predicting gaze-based target selection in augmented reality headsets based on eye and head endpoint distributions. In *Proceedings of the 2023 CHI Conference on Human Factors in Computing Systems*, CHI '23, article no. 283, 14 pages, 2023. doi: 10.1145/3544548.3581042 2

[45] J. Wentzel, M. Lakier, J. J. Hartmann, F. Shazib, G. Casiez, and D. Vogel. A comparison of virtual reality menu archetypes: Raycasting, direct input, and marking menus. *IEEE transactions on visualization and computer graphics*, PP, 2024. doi: 10.1109/TVCG.2024.3420236 2

[46] J. O. Wobbrock, L. Findlater, D. Gergle, and J. J. Higgins. The aligned rank transform for nonparametric factorial analyses using only anova procedures. In *Proceedings of the SIGCHI Conference on Human Factors in Computing Systems (CHI '11)*, pp. 143–146. Association for Computing Machinery, New York, NY, USA, 2011. doi: 10.1145/1978942.1978963 5

[47] R. Xavier, J. L. Silva, R. Ventura, and J. A. P. Jorge. Pseudo-haptics survey: Human-computer interaction in extended reality and teleoperation. *IEEE Access*, 12:80442–80467, 2024. doi: 10.1109/ACCESS.2024.3409449 4

[48] X. Ye and J. Long. Real-time adjustment of tracking offsets through a brain-computer interface for weight perception in virtual reality. *IEEE Transactions on Human-Machine Systems*, 52:855–866, 2022. doi: 10.1109/THMS.2022.3182910 2

[49] D. Yu, T. Dingler, E. Velloso, and J. Goncalves. Object selection and manipulation in vr headsets: Research challenges, solutions, and success measurements. *ACM Comput. Surv.*, 57(4), article no. 98, 34 pages, Dec. 2024. doi: 10.1145/3706417 1, 2

[50] D. Yu, H.-N. Liang, F. Lu, V. Nanjappan, K. Papangelis, and W. Wang. Target selection in head-mounted display virtual reality environments. *JUCS - Journal of Universal Computer Science*, 24(9):1217–1243, 2018. doi: 10.3217/jucs-024-09-1217 2

[51] D. Yu, H.-N. Liang, X. Lu, K. Fan, and B. Ens. Modeling endpoint distribution of pointing selection tasks in virtual reality environments. *ACM Trans. Graph.*, 38(6), article no. 218, 13 pages, Nov. 2019. doi: 10.1145/3355089.3356544 2

[52] D. Yu, X. Lu, R. Shi, H.-N. Liang, T. Dingler, E. Velloso, and J. Goncalves. Gaze-supported 3d object manipulation in virtual reality. In *Proceedings of the 2021 CHI Conference on Human Factors in Computing Systems*, CHI '21, article no. 734, 13 pages, 2021. doi: 10.1145/3411764.3445343 1

[53] R. Yu and D. A. Bowman. Pseudo-haptic display of mass and mass distribution during object rotation in virtual reality. *IEEE Transactions on Visualization and Computer Graphics*, 26(5):2094–2103, 2020. doi: 10.1109/TVCG.2020.2973056 2

[54] A. Zenner and A. Krüger. Shifty: A weight-shifting dynamic passive haptic proxy to enhance object perception in virtual reality. *IEEE Transactions on Visualization and Computer Graphics*, 23(4):1285–1294, 2017. doi: 10.1109/TVCG.2017.2656978 2

[55] A. Zenner and A. Krüger. Drag:on: A virtual reality controller providing haptic feedback based on drag and weight shift. In *Proceedings of the 2019 CHI Conference on Human Factors in Computing Systems (CHI '19)*, pp. 1–12. Association for Computing Machinery, New York, NY, USA, 2019. doi: 10.1145/3290605.3300441 2

[56] Z. Zhao, Y. Li, and H.-N. Liang. Leanon: Simulating balance vehicle locomotion in virtual reality. In *2023 IEEE International Symposium on Mixed and Augmented Reality (ISMAR)*, pp. 415–424, 2023. doi: 10.1109/ISMAR59233.2023.00056 2